



Framboidal and spherulitic pyrite in sediment-hosted ore deposits of Iran

Abdorrahman Rajabi ^{1, *} , Pouria Mahmoodi ², Carles Canet ³, Mohammad Pirouei ⁴, Pura Alfonso ⁵, Amir Mahdavi ⁶, Shojaedin Niroomand ¹ , Mehdi Movahednia ², Sara Momenipour ¹

¹ School of Geology, College of Science, University of Tehran, Tehran 1417614411, Iran

² Department of Geology, Faculty of Sciences, Tarbiat Modares University, Tehran 14115111, Iran

³ Escuela Nacional de Ciencias de la Tierra, Universidad Nacional Autónoma de México, Coyoacán, Mexico City 04150, Mexico

⁴ Department of Petroleum Geosciences, Faculty of Science, Soran University, Erbil, Iraqi Kurdistan, Iraq

⁵ Departament d'Enginyeria Minera, Industrial i TIC, Universitat Politècnica de Catalunya, Av. de les Bases de Manresa 61–73, 08242 Manresa, Spain

⁶ Department of Geology, Faculty of Sciences, University of Birjand, Birjand 9717434765, Iran

Received: 19 December 2022, Revised: 11 November 2023, Accepted: 22 November 2023

© University of Tehran

Abstract

Framboidal pyrite is common in marine sediments and organic matter-bearing sedimentary rocks. It has also been reported in many 'sediment-hosted ore deposits', such as shale-hosted massive sulfide (SHMS) or clastic-dominated Zn-Pb deposits, volcanogenic massive sulfides (VMS), Irish-type Zn-Pb, sediment-hosted stratabound copper (SSC), and sandstone-hosted Pb-Zn and U, as well as in coal deposits, whereas it is absent or rare in some others (e.g., Mississippi Valley Type, MVT). Spherulitic pyrites are more common in Cambrian pyrite-rich SHMS Zn-Pb deposits, hosted in organic matter-rich black shales and siltstones. Framboid textures can be observed in other minerals as well, such as magnetite, hematite, goethite, limonite, magnesium ferrite, chalcocite, cobaltite, digenite, and arsenopyrite. However, it is possible that these non-pyrite framboids are either formed due to the oxidation of pyrite or the replacement of pyrite by other minerals. The recognition of different morphology types of pyrite framboids and spherulites and their relationship with other sulfides are useful in determining the time of formation of these ore deposits, especially in sediment-hosted Zn-Pb mineralizations. Although framboidal pyrite usually has a sedimentary origin, in some sediment-hosted ore deposits (e.g., Koushk, Chahmir, Zarigan, Hossein-Abad, Eastern Haft-Savaran, Tiran, and Irankuh), where it occurs in association with fine-grained sphalerite and galena, and also in the hydrothermal alterations, its origin is influenced by hydrothermal fluid inputs. Whatever its origin, framboidal pyrite allows us to approach the redox conditions of the sedimentary environment, based on a detailed morphometric analysis in each (ore) facies. Suggesting an analogy with modern euxinic sedimentary basins, the large number of framboidal pyrite indicates euxinic to anoxic conditions in the Chahmir, Koushk, Zarigan, Hossein-Abad, Eastern Haft-Savaran, and Ab-Bagh ore deposits, which is consistent with the geochemical proxies of the host rocks.

Keywords: Sediment-Hosted Ore Deposits, Sedimentary-Exhalative (SEDEX), Euxinic, Anoxic, Mineral Texture, Framboids, Spheroidal.

* Corresponding author e-mail: rahman.rajabi@ut.ac.ir

Introduction

Pyrite is a common sulfide mineral in ore deposits, and displays different textures and shapes, occurring in various geological environments associated with other sulfides. This mineral is well known to geologists involved in the study of ore deposits, and different thermodynamic and geochemical models are available to deduce its origin. Pyrite is formed in a wide range of physicochemical conditions (e.g., $Eh \approx -6$ to $+0.2$ v, $pH \approx 2 - 9.7$, $fO_2 < -60$ bar, $fS_2 > -35$ bar, in Fe-O-S system at about 20° to 540° C; Rickard, 2006, 2012, 2019a) of sedimentary, magmatic, metamorphic and hydrothermal environments. The occurrence and textures of pyrite in any environment depend on the temperature, Eh, and pH conditions, and its abundance in the availability of Fe and S to form pyrite. The presence of pyrite as the dominant or one of the major sulfide minerals in ore deposits represents the different conditions governing the formation of these mineralizations.

Pyrite could occur in different stages of mineralization in sediment-hosted ore deposits, forming distinctive structures and textures as massive (Figure 1a,b), banded (Figure 1c), laminated (Figure 1d-f), vein-veinlets (Figure 1g), diagenetic nodules (Figure 1h), disseminated (Figure 1i), colloform (Figure 1j), framboidal (Figure 1k), spheroidal (spherulite, Figure 1m,n), bubble (Figure 1n,o), and replacement; each of them indicates special environmental conditions or mineralizing processes. Among them, framboids (Figure 2a,b) and spherulites (Figure 2c,d) are the most common textures in many sediment-hosted ore deposits, as well as modern anoxic marine sediments such as organic matter-rich muds, black shales and siltstones, and even in some carbonates. The term "framboids" was first used by Rust (1935) for raspberry-like aggregates of very fine pyrite grains, derived from the French word *framboise*. Pyrite framboids in sediments commonly form by bacterial sulfate reduction (BSR), when iron is available in the depositional environment (Ohfuji & Rickard, 2005). Jakobsen and Postma (1999) reported framboidal pyrite in shallow sandy aquifers, where the BSR rate is lower than in marine sediments.

Besides pyrite, framboids have also been reported for magnetite (Suk et al., 1990), hematite (Lougheed & Mancuso, 1973), goethite, limonite, magnesium ferrite (Taylor, 1982), and even chalcocite, digenite (Sawlowicz, 1990) and arsenopyrite (Sawlowicz, 1993). Most of the non-pyrite framboids could be the result of oxidation products of pyrite (hematite, limonite), or replacement of pyrite with other minerals (e.g., magnetite, chalcocite, digenite, and arsenopyrite).

Pyrite in the form of framboids is one of the most common sulfides in many sediment-hosted ore deposits, especially in shale-hosted massive sulfide (SHMS) or clastic-dominated Zn-Pb (e.g., HYC and Mt Isa, Australia), Irish-type Zn-Pb (e.g., Tara Deep, Navan, and Island Pod, Ireland; Irankuh and Mehdiabad, Iran), sediment-hosted stratabound Cu (SSC), sandstone-hosted U (SSU), sandstone-hosted Pb-Zn, as well as in volcanogenic massive sulfide (VMS) deposits (like Rio Tinto, Spain), where the relationship between framboidal pyrite and ore genesis generated considerable interest (e.g. Sangster & Bajocine, 1996; Large et al., 1998; Wilkinson, 2003; Wilkinson et al., 2005; Mahdavi, 2008; Rajabi, 2008; Rajabi et al., 2012b, 2015a,b, 2020, 2023; Piercey, 2015; Gadd et al., 2016; Magnall et al., 2016; Yesares et al., 2019; Movahednia et al., 2020a,b; Mahmoodi et al., 2018, 2021, 2023; Mahdavi and Rajabi., 2023). The presence of framboidal pyrite in non-sedimentary environments is not unusual; even the presence of this particular pyrite textural variety has been reported in some igneous rocks (Steinike, 1963; Love & Amstutz, 1969) and some non-sedimentary ore deposits, such as epithermal Au-Ag deposits (Rosua et al., 2003).

Various genetic models for the formation of sedimentary ore deposits have been developed. A key aspect of these models is the textures and mineral assemblages that help us to determine the evolution and relative timing –paragenesis- of ore minerals deposition.

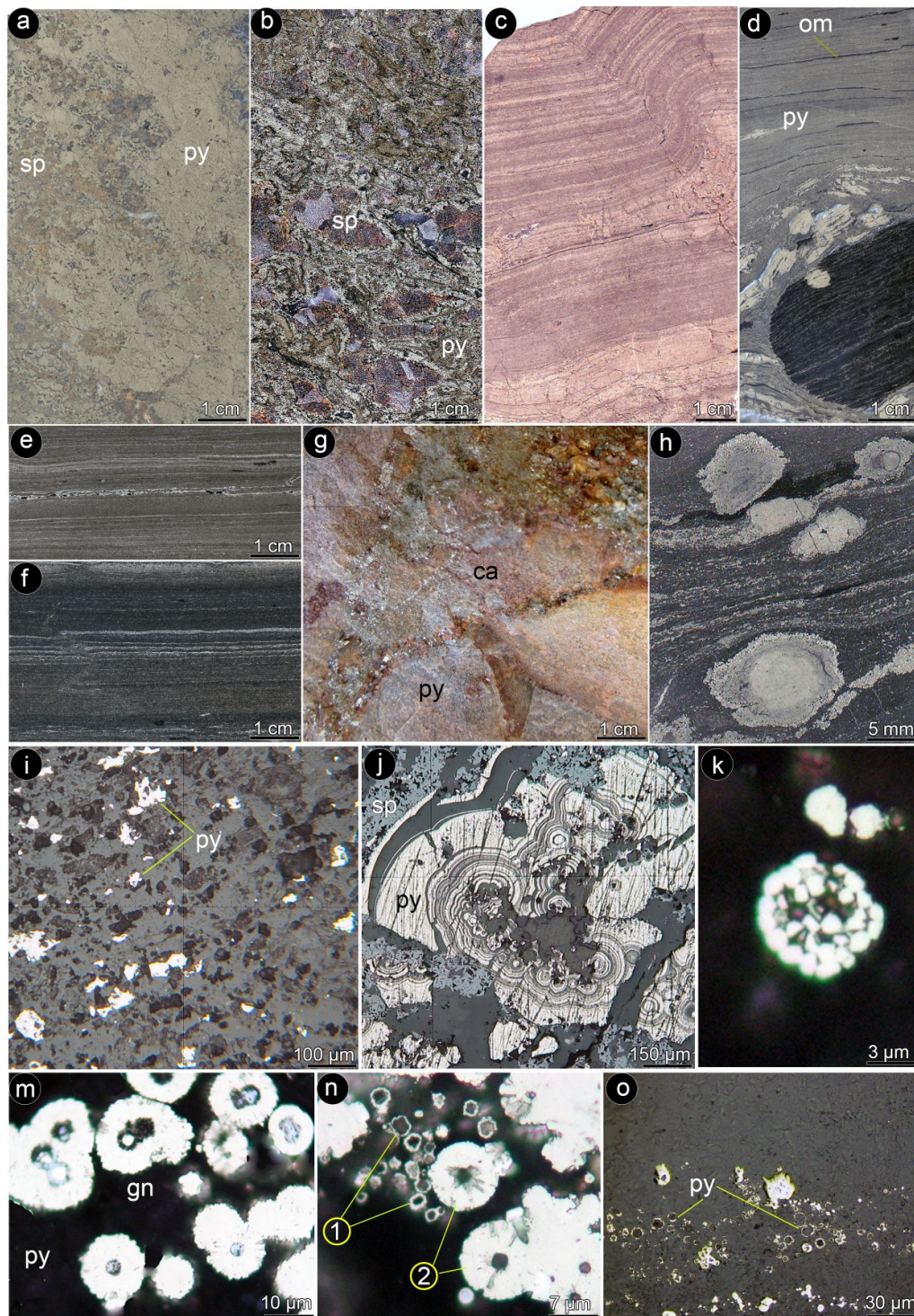


Figure 1. Different pyrite structures and textures in sediment-hosted Zn-Pb deposits. a, b) Massive pyrite which is replaced with sphalerite, Chahmir (a) and Koushk (b) deposits; c) Banded massive pyrite in bedded ore of the Koushk deposit. d, e, f) Laminated pyrite in black siltstones of the Chahmir (d) and Koushk (e, f) deposits; g) Pyrite veins in dolomitic limestone of the Ab-Bid deposit. h) pyrite nodules and laminated pyrite in black shale, Chahmir deposit; i) disseminated coarse-grained pyrite in siltstone, Central Iran; j) Replacement of colloform pyrite with sphalerite, Chahmir deposit; k) Framboidal pyrite in the host black shale of the Chahmir deposit. m, n) Bubble texture of pyrite (1) and pyrite spherulites (2) in Chahmir deposit. o) Bubble texture of pyrite in a lamina, Koushk deposit. py: pyrite, gn: galena, sp: sphalerite

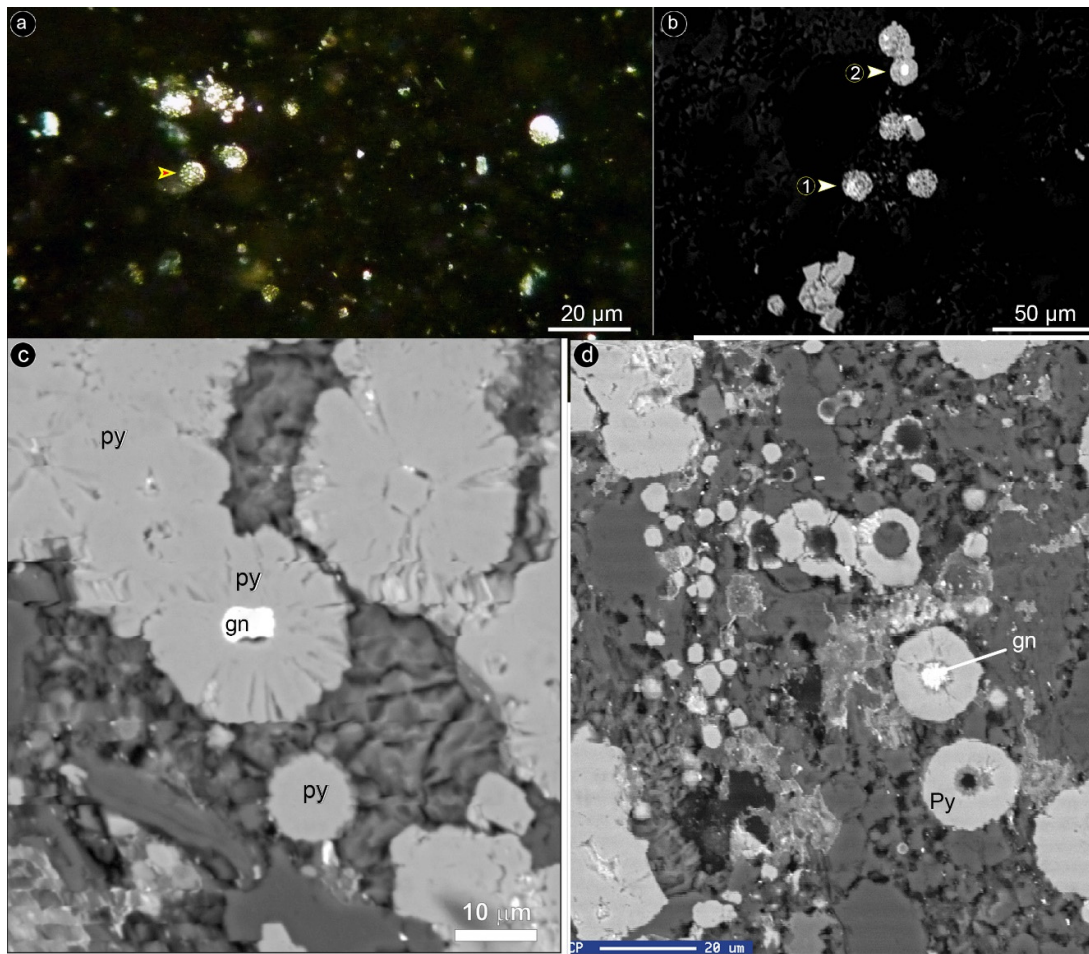


Figure 2. a) Microscopic photograph of pyrite framboids in the Hossein-Abad deposit. b) Back-scattered electron (BSE) photographs of framboidal pyrite in the Eastern Haft-Savaran. c and d) Pyrite spherulites in the Chahmir deposit. py: pyrite, gn: galena

Also, determining the redox conditions controlling mineralizing processes is particularly relevant in investigating the genesis of sediment-hosted ore deposits. In this contribution, an attempt has been made to investigate the morphology and textural relationship of framboidal pyrite as a tool in determining the conditions governing the formation of some selected sediment-hosted Zn-Pb and Cu deposits of Iran and the role of pyrite framboids in the formation of ores.

Methods

For this study, 85 samples were collected from the sulfide-bearing facies of Iranian sediment-hosted ore deposits grouped in five different types: (a) Koushk, Zarigan, and Chahmir, Hossein-Abad, Ab-Bagh and Western Haft-Savaran, SHMS Zn-Pb type; (b) Ab-Bid, Tarz, Ahmadabad, Talkhab, and Zenoghan, MVT; (c) Mehdiabad, Farahabad, Mansourabad, Anjireh-Tiran, Robat, Lakan, Eastern Haft-Savaran, and Irankuh, Irish type; (d) Markesheh, Bagh-Pahlevan, Esmail-Abad, Kuh-e-Sargerd, Chahbouk and Ark, SSC (Figure 3). Weathered intervals and samples were avoided during sampling.

Pyrite textural characteristics were examined in polished and thin-polished sections using an optical microscope, scanning electron microscopy (SEM) with back-scattered electron (BSE), and electron microprobe analysis (EPMA) at the University of Tehran, and the National University of Mexico (UNAM). A total of 4188 pyrite framboids have been sized and

photographed. Framboidal pyrite's diameter was measured across each section until a population of more than 100 was achieved. The minimum, arithmetic and geometric mean, maximum diameter, arithmetic and geometric standard deviation of diameter, and the percentage of pyrite framboids were calculated in each sample. Also, the details of the morphology and aggregates of the pyrite framboids and spherulites were examined using SEM and EPMA with BSE images.

Textural characterization of pyrite framboids and spherulites

In the studied sediment-hosted ore deposits, framboids are densely packed, raspberry-like spherical aggregates of micron-sized subhedral crystals that range from a few microns to several tens of microns in diameter. In turn, framboids make larger accumulations up to hundreds of micrometres. In SHMS Zn-Pb deposits framboids occur as disseminated, lenses and nodules, laminae and bands, alternating with the detrital laminae (black shales and siltstones). The above has been observed in the Koushk and Chahmir deposits (Figures 1d-f, k-n, 4), hosted in the Early Cambrian volcano-sedimentary sequence (Rajabi et al., 2015a,b, 2020), and in the Hossein-Abad, and Ab-Bagh deposits (Figure 5; Jurassic shales and sandstones of the Sanandaj-Sirjan Zone; Mahmoodi et al., 2018, 2021; Movahednia et al., 2020a). Pyrite spherulites are common in Early Cambrian SHMS Zn-Pb deposits and are associated with pyrite framboids laminae. They either have no inner structure or are composed of globules and radial-bladed pyrite (Figure 4).

While in some carbonate-hosted (Irish-Type; Rajabi, 2022; Rajabi et al., 2023; Khan Mohammadi et al., 2023) Zn-Pb deposits, in which the host rocks are organic matter-rich, such as Irankuh (Boveiri Konari et al., 2017, 2018; Rajabi et al., 2012b; 2019a; 2023; Afzal et al., 2022), and Eastern Haft-Savaran (Mahmoodi et al., 2019, 2023) in Early Cretaceous carbonates of the Sanandaj-Sirjan zone, framboidal pyrite generally occurs as disseminated (Figure 6), small nodules and rarely fine discrete laminated textures.

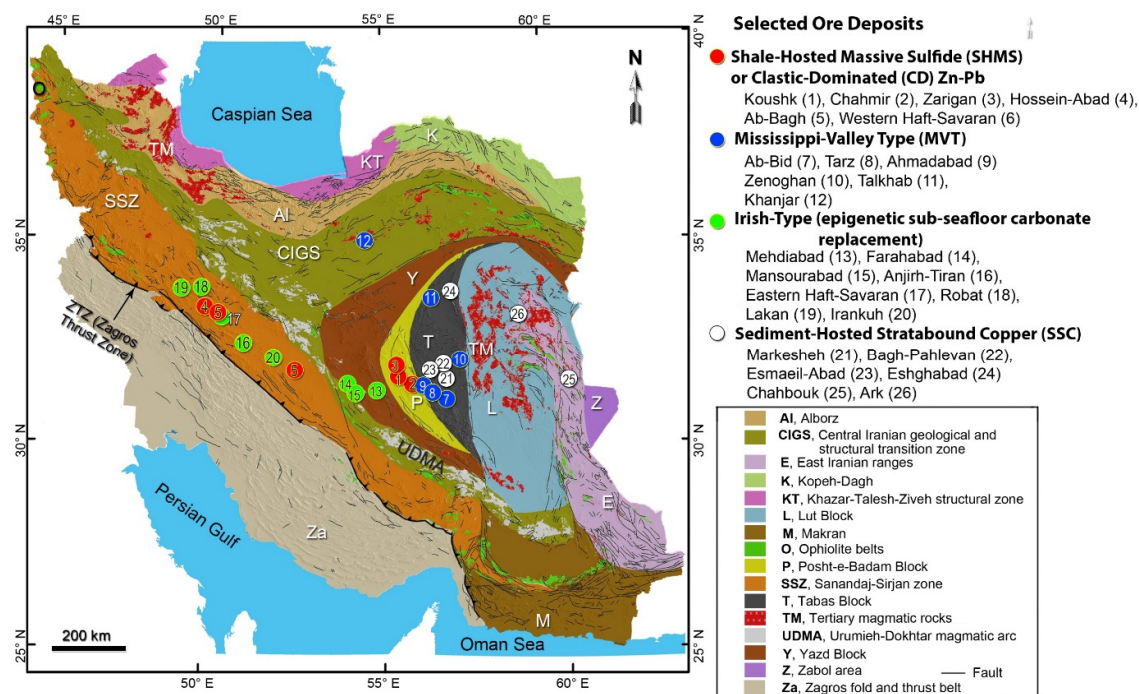


Figure 3. Location of the selected sediment-hosted ore deposits on the structural map of Iran (based on Aghanabati, 1998; modified after Rajabi et al., 2019b)

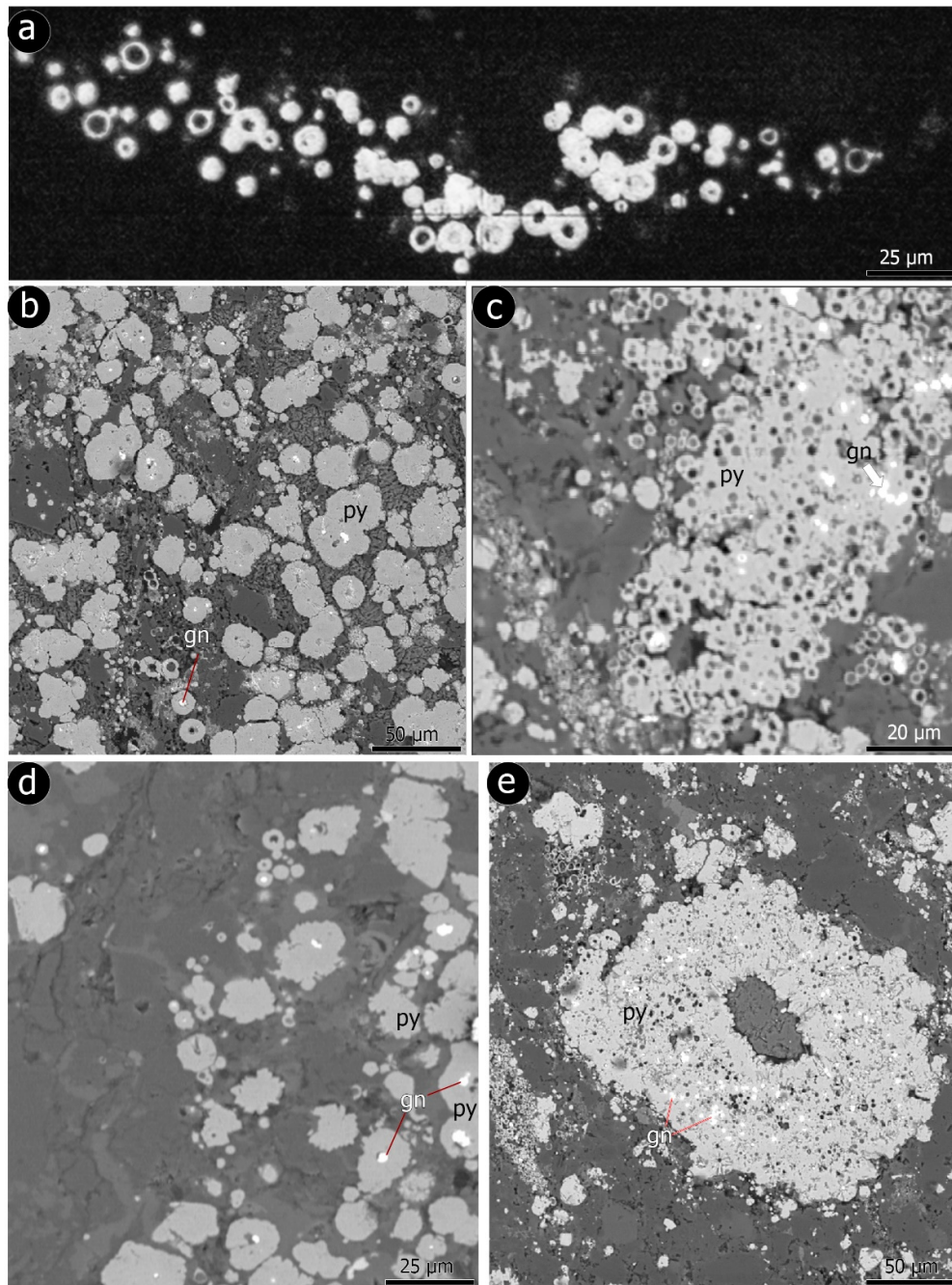


Figure 4. Microscopic (a) and Back-scattered electron (BSE) photographs (b-e) of pyrite spherulite (with atoll structures) accumulations in Early Cambrian black shales and siltstones of the Koushk and Chahmir SHMS Zn-Pb deposits. py: pyrite, gn: galena.

In VMS deposits (e.g., Nokuhi, Dorrin) and SSC deposits (e.g., Markesheh, Bagh-Pahlevan; Mahdavi, 2008; Mahdavi et al., 2011; Rajabi et al., 2019b; Mahdavi & Rajabi, 2023), the framboidal pyrite is moderately common and occur as small accumulations associated to organic matter and usually are replaced by other sulfides. In particular, in the SSC deposits, pyrite framboids occur associated with fossil plant remains in sandstones of the Late Jurassic red beds (Garedu Formation). In these deposits, chalcocite is a major sulfide and replaced the framboidal pyrite (Figure 7), in what can be described as “pseudo-framboids” (Mahdavi & Rajabi, 2023).

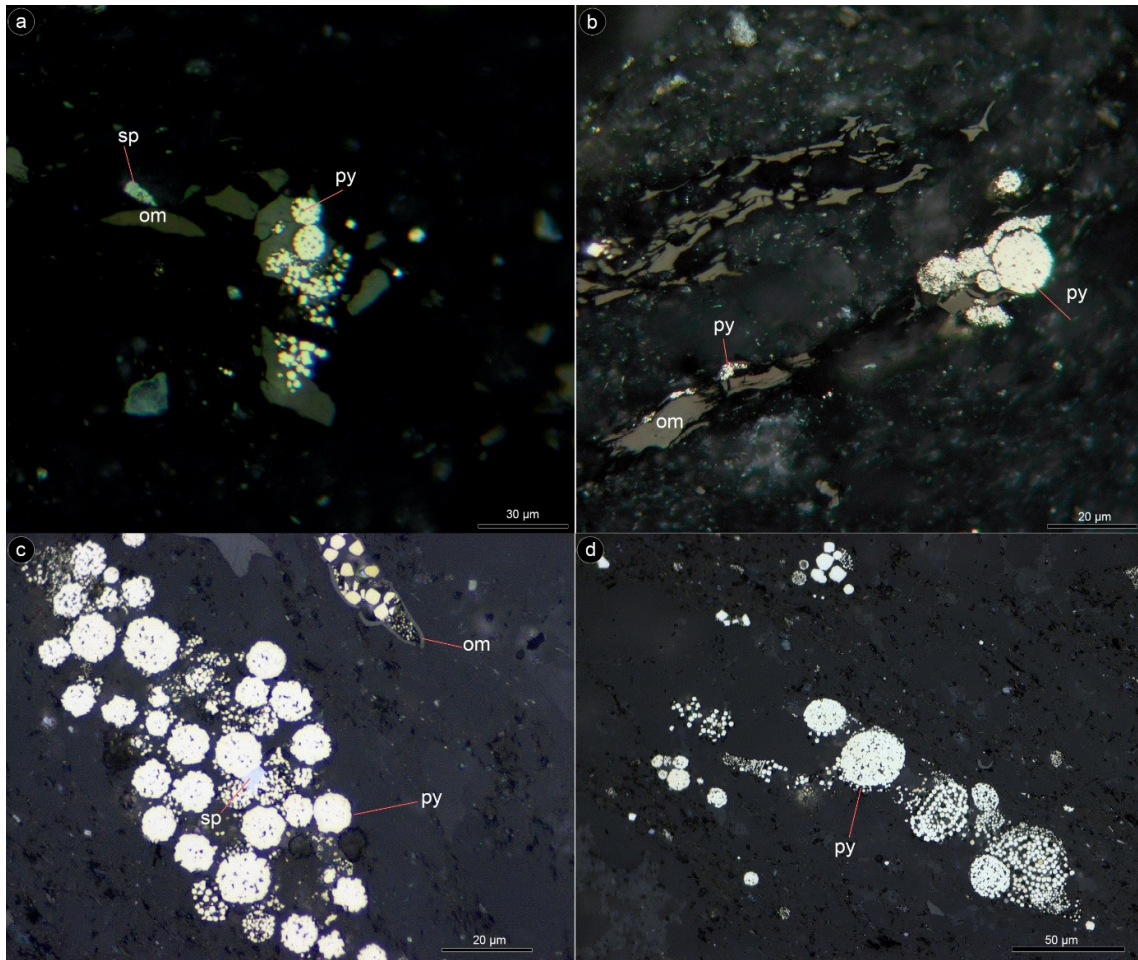


Figure 5. Microscopic photographs of pyrite framboid accumulations with organic matter in Late Jurassic black shales of the Hossein-Abad (a, b) and Ab-Bagh (c, d) SHMS Zn-Pb deposits. py: pyrite, gn: galena, sp: sphalerite, om: organic matter

In Koushk, and Chahmir SHMS Zn-Pb deposits, hosted in Early Cambrian black shales and siltstones, the first generation of pyrite constitutes over 40% of all pyrite in bedded ore facies of these deposits. It occurs as 2 to 6 µm euhedral to subhedral cubic crystals, framboids, fine-grained spherulites (Figure 4), and tightly packed round to lenticular aggregates of polyspherulites (Figure 4c,e) and ‘bubble’ textures. Fine-grained crystalline pyrite and framboids are minor components of the black shales and siltstones of the Koushk member in the host basin of these SHMS deposits, but these types of pyrite along with spherulites are quite abundant in the bedded ore of these mineralizations (5–35 vol%). Spherulite texture is the most common form of pyrite in bedded ores and occurs in disseminated and laminated textures. Accumulation of these spherulites, along with minor microeuhedral pyrites, makes loosely rounded lenticular aggregates (Rajabi et al., 2020). Single spherulites are more common than framboids in the bedded ore; moreover, euhedral fine-grained pyrite or galena may occur at the core of some spherulites (Figure 4). Single spherulites are generally <2-7 µm in diameter (less commonly up to 15 µm in diameter) and are composed of radiating fibrous pyrite. Framboids, microeuhedral, and spherulite pyrite usually show close spatial relationships and occur as random dissemination, irregular clusters, and also laminae in the bedded ore of these deposits. These pyrite textural varieties are primary kernels for subsequent pyrite growth and, are grouped into the first generation of pyrite in the SHMS deposits (Rajabi et al., 2020). At the Koushk and Chahmir deposits, the fine-grained sphalerite is characteristically associated with

ehedral pyrite crystals, framboids, and spherulites, and it occurs as disseminated grains dominantly in sphalerite-pyrite- and rarely sphalerite-galena- rich laminae (Rajabi et al., 2012a; 2020).

Unlike the Early Cambrian SHMS deposits, in Late Jurassic Hossein-Abad, Ab-Bagh, and Western Haft-Savaran deposits (Mahmoodi et al., 2018; Movahednia et al., 2020), pyrite almost exclusively occurs in the form of framboids, which also are common in Irankuh, Tiran, and Eastern Haft-Savaran deposits, hosted in Early Cretaceous carbonate rocks, with minor siltstones and shales (Yarmohammadi et al., 2016; Boveiri Konari et al., 2018; Mahmoodi et al., 2018, 2023; Movahednia et al., 2020; Rajabi et al., 2023). In these deposits, very fine-grained sphalerite and galena are associated with framboidal pyrite and show a close genetic relationship with each other (Figure 6).

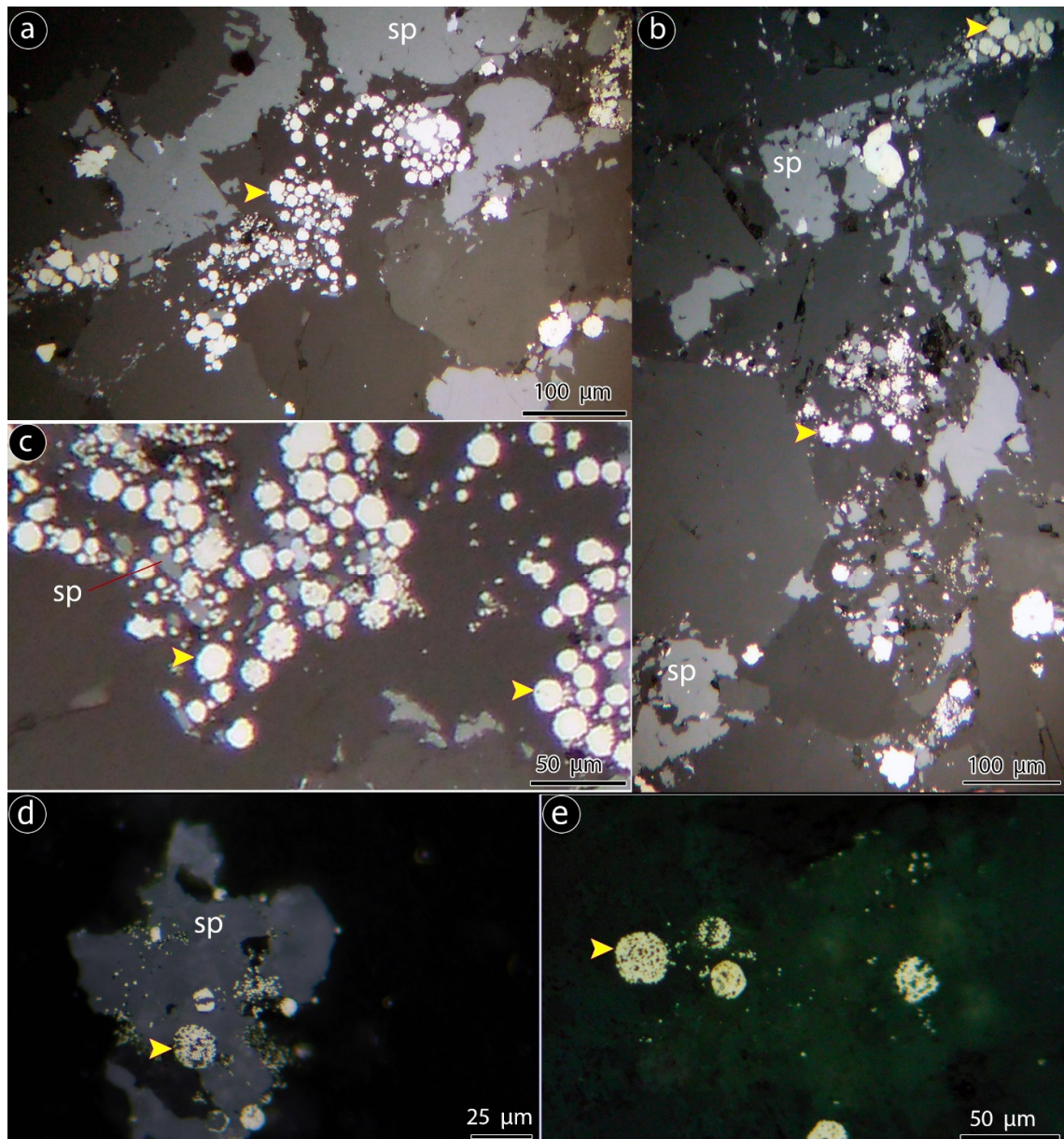


Figure 6. Reflected light photomicrographs of pyrite framboids (yellow arrow) and sphalerite in Irankuh (a-c) and Eastern Haft-Savaran (d, e) deposits in Early Cretaceous organic matter-bearing carbonate rocks. In d pyrite framboids are replaced with sphalerite. py: pyrite, sp: sphalerite

In some of these deposits, a later and coarse-grained sulfide (sphalerite and galena) replacement event is observed. In the Hossein-Abad deposit, framboidal pyrite forms ellipsoidal, circular, and polyframboidal aggregates. At the Irankuh deposit, the framboidal pyrite often displays circular, homogeneous, and polyframboidal forms. In contrast, in the Eastern Haft-Savaran deposit, pyrite has variable sizes and even is seen as defective forms.

Discussion

Pyrite framboids and the paleo-redox conditions of the sedimentary environments

In modern sedimentary basins, pyrite framboids occur as accumulations on the restricted iron-reduction, redox boundary. As a result of the diversity of framboids' environments, various genetic models and morphology schemes for pyrite framboids have been developed, as reviewed, for example, by Love (1971), Stene (1979), Sawlowicz (1993), Wilkin et al. (1996), Wilkin & Barnes (1997), Wignall & Newton (1998), Ohfuji & Rickard (2005), Wignall et al. (2005), Scott et al. (2009), Bond & Wignall (2010), Prol-Ledesma et al. (2010), Gallego-Torres et al. (2015) Zhao et al. (2018), Liu et al. (2019; 2022), and Rickard (2019b, 2021). In sedimentary environments, framboidal pyrites are mainly considered syngenetic or early diagenetic components (Skei, 1988; Love and Amstutz, 1966; Berner, 1970; Rajabi et al., 2020). However, they can also form during late diagenesis (Menon, 1967; Canfield and Berner, 1987). In addition, Rickard (1970) suggested that fine-grained framboids could be found floating in the water column, and Degens et al. (1972) and Middelburg et al. (1988) reported framboids in anoxic and euxinic water columns. Wilkin et al. (1996), and Suits & Wilkin (1998) suggested that pyrite framboids defect growing in the fully anoxic conditions of the underlying sulfate-reduction zone where crystalline pyrite forms. Framboidal pyrite aggregates are indicative of oxygen-poor or anoxic sedimentary environments (Wignall et al., 2005), and their formation is generally limited to the euxinic water column, and below the sediment-water interface (Sawlowicz, 2000), and they can grow during the first stages of early diagenesis (Wilkin et al., 1996).

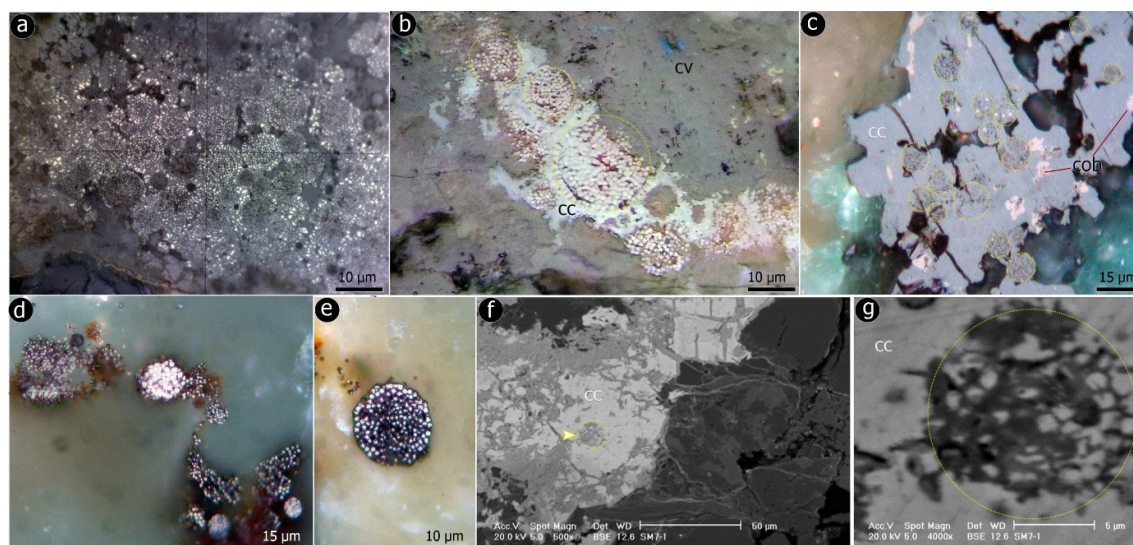


Figure 7. a) Reflected light photomicrographs of pyrite framboids in Ark SSC deposit. b, c) Replacement of pyrite framboids with chalcocite and cobaltite in Ark (b), and Markesheh (c-d) SSC deposits. e) Pseudo-framboids of chalcocite, representing replacement of pyrite framboid with chalcocite in SSC deposits, Central Iran. f, g) Back-scattered electron (BSE) photographs of framboids that are replaced with chalcocite, Markesheh deposits. cc: chalcocite, cob: cobaltite

However, Raiswell & Berner (1985) suggested that diagenetic pyrite forms within the sediment with anoxic conditions, under an oxic water column, but some studies (e.g., Rajabi et al., 2020) show that framboids can form in both anoxic and dysoxic environments.

Framboidal pyrite can display a variation of morphology, size, isotopes, and trace element compositions. The stability and preservation of framboidal and spherulitic pyrite depend on (1) prevention of framboids to recrystallize during diagenesis, (2) interruption in the supply of one of the main reactant compounds in the fluid (iron or H₂S), (3) formation in an oxygen-poor or anoxic environment and maintaining this condition. The presence of organic matter pods can protect the framboids from alteration and weathering (Kribek, 1975). A low concentration of chemical compounds of pyrite prevents a rapid formation and, as a result, euhedral pyrite is formed instead of framboids (Sawlowicz, 1993).

Organic matter is not required for framboid formation (Sawlowicz, 1993), but it plays an effective role in the formation and maintenance of framboidal pyrite with different sizes by their accumulations (Figure 5a,b). Framboidal pyrite that is formed in the absence of organic matter quickly undergoes recrystallization to give place to euhedral pyrite grain. In experimental studies, in the presence of organic matter, framboids form separated particles that are relatively durable (Sawlowicz, 1993).

In euxinic bottom water with free H₂S, framboids of uniform, small size, along with very fine-grained single cubic grains, crystallized in the water column and then settled to the basin floor (Wilkin et al., 1996). These framboids are unable to attain larger size until they sink below the iron-reduction zone and cease to grow (Bond & Wignall, 2010). As a consequence, in euxinic conditions, pyrite forms tiny framboids whose size distributes in a narrow range (Wignall & Newton, 1998; Table 1). In contrast, under dysoxic to anoxic conditions, the bottom water is weakly oxygenated and framboids form in the sediment–water interface, where their size is governed by the local availability of iron and sulfur; as a result, their sizes are more variable and usually larger (Wilkin et al., 1996). In this condition, their average diameters are between 6 and 10 μm.

Using the framboid size-frequency measurements as a paleo-environmental indicator faces limitations because it depends on the relationship between pyrite framboid sizes and modern euxinic and non-euxinic environments, but none of them sampled from the water column (Rickard, 2019b, 2021). However, Wilkin et al. (1996) and Wignall & Newton (1998) suggested that there is a strong relationship between the mean and standard deviation of the diameter size of framboids and the redox conditions of the sedimentary environments (Table 1), but Rickard (2019b), based on the geometric mean size of the framboids, represented that there is a significant overlap between framboid sizes in syngenetic and diagenetic conditions.

Table 1. Characteristics of pyrite framboids in different redox conditions during deposition (after Bond & Wignall, 2010)

Redox conditions	Framboid characteristics
Euxinic	Very fine-grained small framboids (mean 3–5 μm), abundant spherulites in the presence of organic matter, with a narrow size range.
Anoxic	fine-grained small framboids and spherulites (mean 4–6 μm), abundant, with a few, larger framboids.
Lower dysoxic (weakly oxygenated)	Mean 6–10 μm with some larger framboids spherulites, and crystalline pyrite.
Upper dysoxic (partial oxygen)	Framboids are moderately common to rare, with a broad range of sizes (6–50 μm). Majority of pyrite as crystals
Oxic	No framboids of spherulites, with rare pyrite crystals.

However, the application of additive statistics to framboid populations and their arithmetic means and standard deviations are commonly used to determine the oxygenation states of paleo-sedimentary environments, but this method predicts an impossible subset of framboids with negative diameters in these basins (Rickard, 2019b). So, in this research, we used both the arithmetic and geometric statics parameters (based on Rickard, 2019b) to compare the results. The results of statistical parameters and meta-analyses of framboid sizes are listed in Table 2, and summarized in Figure 8, for the Koushk, Chahmir, Hossein-Abad SHMS, and Eastern Haft-Savaran Irish-type Zn-Pb deposits. According to the average parameters (mean) and standard deviation (St. Dev.) obtained in the host siltstones of these deposits and based on the criteria provided by Wilkin et al. (1996) and Bond & Wignall (2010), the size of the framboidal pyrites is indicative of anoxic to lower dysoxic environments (Figure 9). However, the calculation of the geometric parameters (meta-analyses) based on the criteria provided by Rickard (2019b) shows a small variation in geometric standard deviations of the framboidal pyrites in the selected ore deposits. The results show that all framboids in these ore deposits have geometric standard deviations between 1.4 to 1.9, and this small variation is not discriminable in euxinic and non-euxinic environments (Rickard, 2021; Figure 9).

Table 2. Summary of database for framboid meta-analyses in some selected SHMS and Irish-type Zn-Pb deposits

Ore Deposit	Ore Deposit Type	Number	Arithmetic Mean	Geometric Mean	Arithmetic St. Dev.	Geometric St. Dev.	Variance	Max	Min
Koushk	SHMS	349	3.44	2.72	3.52	1.85	12.40	32	1
Chahmir	SHMS	347	3.78	2.94	3.93	1.89	15.44	31	1
Hossein-Abad	SHMS	1004	5.52	4.83	3.12	1.69	9.73	20	1.00
Eastern Haft-Savaran	Irish-type	2488	10.23	9.53	4.04	1.46	16.33	50	3.00
Irankuh	Irish-type	533	11.78	10.64	3.63	1.35	15.9	48	2

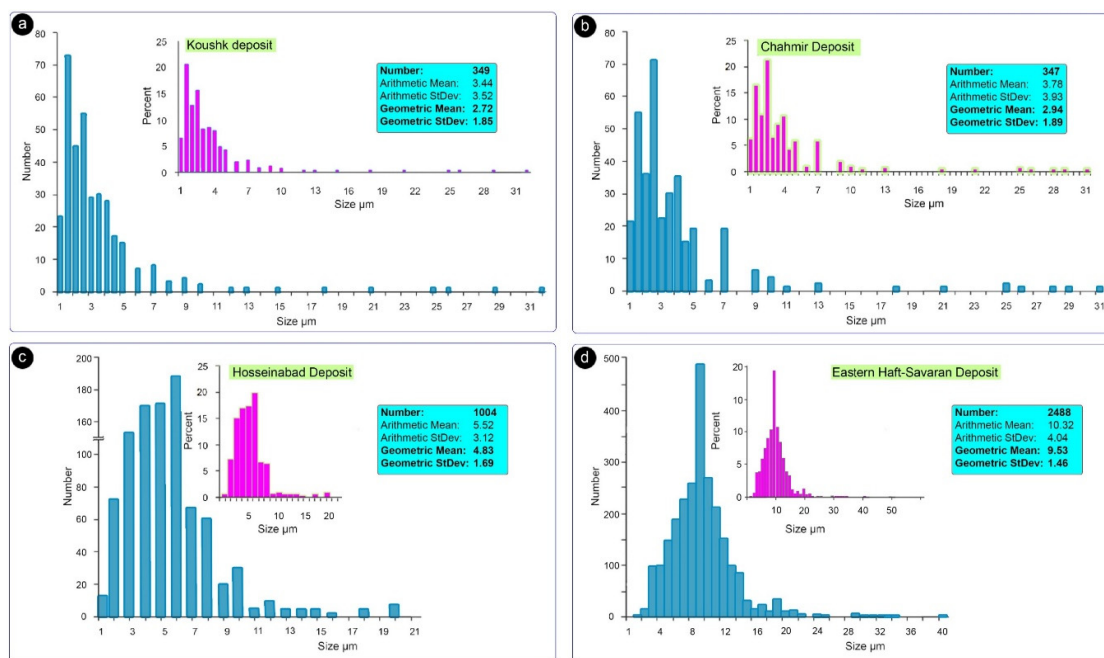


Figure 8. Size-frequency plot of framboidal pyrite populations from the host rocks of the Koushk (a), Chahmir (b), Hossein-Abad (c), and Eastern Haft-Savaran deposits

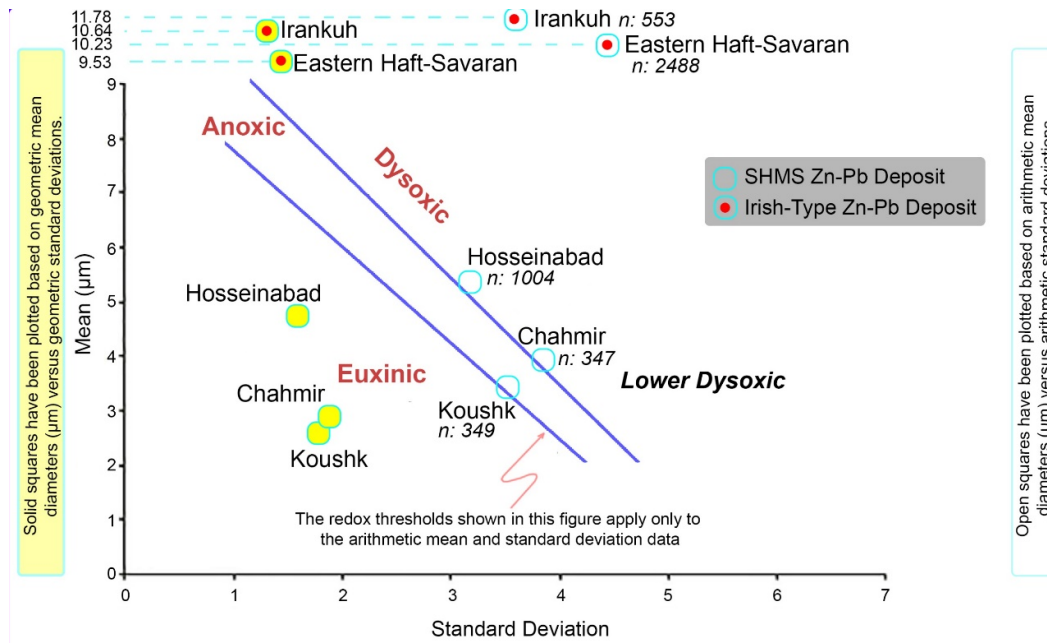


Figure 9. Plots of geometric mean diameters versus geometric standard deviations (unitless, solid square) superposed on the arithmetic mean versus standard deviation plot (open squares) of pyrite framboid data from the Chahmir, Koushk, Hossein-Abad SHMS Zn-Pb, Irankuh and Eastern Haft-Savaran (Irish-type) Zn-Pb deposits. The boundaries between fields for euxinic, anoxic and dysoxic environments in this figure apply only to the arithmetic mean and standard deviation (from Wilkin et al., 1996)

An adequate sedimentary environment characterized by anoxic conditions is a controlling factor in forming and preserving SHMS and VMS deposits (Betts et al., 2003; Goodfellow & Lydon, 2007; Rajabi et al., 2015a,b). The pyrite framboids laminae in the bedded ore facies and host rocks of these deposits imply ore deposition in low-energy and deep-water environments. The presence of a large number of framboids in SHMS, Irish-type and VMS deposits reflects the euxinic to anoxic conditions of the host rock depositional environments. In addition, the alternation of organic matter-rich laminae with sulfide-rich laminae represents an oxygen-poor depositional environment (Cooke et al., 2000) in these ore deposits.

Trace element geochemistry of non-mineralized organic-rich siltstones of the Koushk member (in the Koushk and Chahmir areas) indicates anoxic conditions for the sedimentary environment in which sulfide minerals were deposited. In fine-grained detrital sedimentary environments, anoxic conditions also are characterized by high V/Cr ratios and V/(V + Ni) ratios between 0.5 and 0.9 (Calvert & Pedersen, 1993; Jones & Manning, 1994; Hoffman et al., 1998). Figure 10a shows that the ore-bearing sedimentary rocks of the Ab-Bagh, Koushk and Chahmir deposits were formed under anoxic conditions. In a V/Mo versus Mo plot (Piper & Calvert, 2009; Xu et al., 2012), all analyzed samples of the Ab-Bagh deposits plot across the anoxic and suboxic boundary, and samples from the Koushk and Chahmir deposits represent anoxic to euxinic depositional conditions (Figure 10b).

Pyrite Framboids in sediment-hosted ore deposits

Detailed petrography studies in selected sediment-hosted Zn-Pb and copper ore deposits show the association of pyrite framboids with hydrothermal ore minerals of some deposits (e.g., Koushk, Chahmir, Ab-Bagh, Irankuh); in contrast, this association is not seen in others (e.g., Talkhab, Ab-Bid, Khanjar).

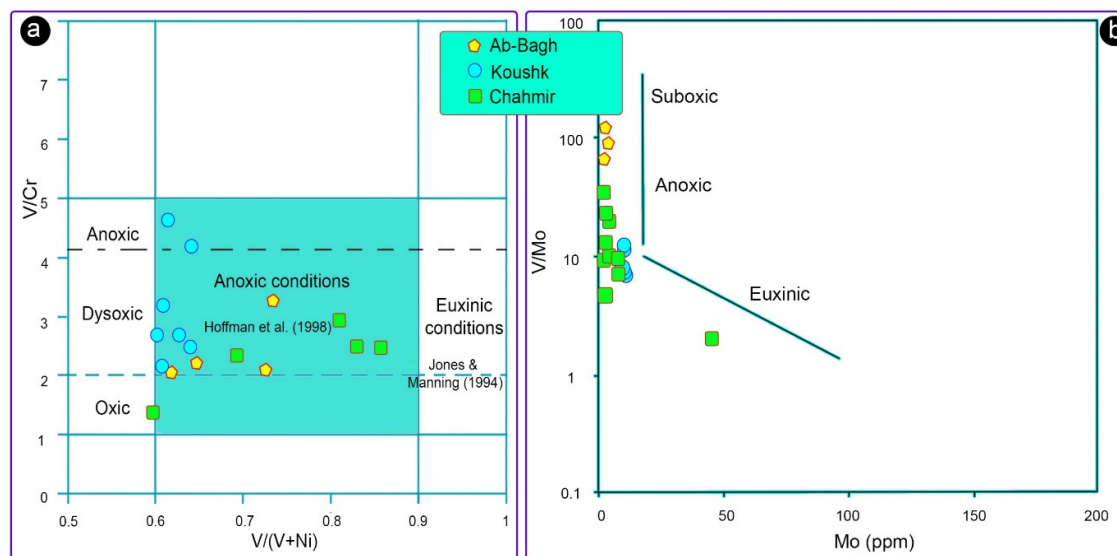


Figure 10. Paleo-redox plots for SHMS Zn-Pb deposits. a) Bivariate plot of the black siltstone samples from Koushk, Chahmir, and Ab-Bagh deposits in the diagram V/Cr versus V/(V + Ni) from Sáez et al. (2011). Limits of environmental conditions from Jones & Manning (1994) and Hoffman et al. (1998). b) V/Mo versus Mo paleo-redox plot modified after Piper & Calvert (2009) and Xu et al. (2012). Data from Rajabi et al. (2015) and Movahednia et al. (2020)

In the Koushk, Chahmir, Irankuh, Tiran, Hossein-Abad and Western- and Eastern Haft-Savaran deposits pyrite framboids are associated with fine-grained hydrothermal sulfides (galena and sphalerite). This association indicates the role of ore-forming hydrothermal processes in their formation (Table 3). The size of the framboids in the Koushk, Chahmir, and Hossein-Abad indicates that the majority of pyrite formed in the water column and some of them were probably formed in the porewaters of the sediments, beneath the sediment-water interface, during the early diagenesis under anoxic to lower dysoxic conditions (Rajabi et al., 2015b), while in the Goshfil deposit (in Irankuh mining district; Boveiri Konari et al., 2017) and Eastern Haft-Savaran (Mahmoodi et al., 2018) pyrite formed at the sediment-water interface, in un lithified black mud with anoxic porewater. Homogeneous framboids are formed by a rapid reaction in a homogeneous environment with sufficient reactants of iron monosulfide and sulfur (Sawlowicz, 1993). Therefore, polyframboids with different sizes observed in the Irankuh and Eastern Haft-Savaran deposits occurred due to the inhomogeneous distribution of iron in the environment (Stene, 1979). Also, the formation of annular pyrite in the Eastern Haft-Savaran deposit was probably because of the first stages of the development of framboids in a depositional environment with low availability of iron and sulfur (Love, 1967). The formation of pyrite framboids begins from the surface of a gel globule and continues toward the core. The presence of an internal cavity at the centre and the formation of annular pyrite probably is due to the low availability of iron and/or sulfide (Sawlowicz, 1993). The association of framboids with annular pyrites in the Eastern Haft-Savaran deposit represents that the high rate of formation of framboids decreased the availability of iron and sulfur monosulfide.

The presence of hydrothermal sulfides such as galena, sphalerite, and chalcopyrite associated with framboidal pyrite has been reported in some SHMS and Irish-type Zn-Pb deposits. In the Howards Pass (in Canada) and the Koushk deposits, sphalerite forms fine-grained disseminated to laminated sulfides, and as mixed sphalerite-framboidal pyrite laminae (Gadd et al., 2016; Rajabi et al., 2020). The formation of these assemblages is attributed to the first stage of mineralization and is related to BSR (Rajabi et al., 2015b; Gadd et al., 2016). The presence of interstitial chalcopyrite in pyrite framboids has been reported in the Tasmanian Folded Belt

base metal deposits. In these deposits, the formation of chalcopyrite has been considered to take place shortly after the formation of framboidal pyrite (England & Ostwald, 1993).

Detailed petrography studies in the Koushk and Chahmir SHMS Zn-Pb deposits represent two major paragenetic generations of sulfide mineralizations at the bedded ore facies, (1) stage I comprising very fine-grained ($< 6 \mu\text{m}$) framboids, spherulite pyrite, associated with minor fine-grained disseminated sphalerite, and galena; and (2) Stage II is composed of a diagenetic intergrowth of coarse-grained framboids and spherulite pyrite, packed polyspherulite aggregates, and pyrite nodules replacing diagenetic barite and carbonate nodules, and are followed with coarse-grained sphalerite and galena that replace former sulfides and barite, deposited as disseminated, laminated, and sulfide-rich banded textures. Data presented by Gadd et al. (2016) and Rajabi et al. (2020) in the SHMS deposits are against a syngenetic, purely synsedimentary model, proving that these deposits formed predominantly during the diagenesis in the uppermost unlithified sediment pile.

The formation of galena and sphalerite as interstitial growths in framboidal pyrite (Figures. 2c,d, and 4; in anoxic to dysoxic environments) of the Chahmir, Koushk, Hossein-Abad, and western Haft-Savaran deposits indicates that the formation of framboidal pyrite, as the first generation of sulfide during mineralization, continue with the formation of hydrothermal fine-grained sulfides in early diagenesis. This stage of mineralization includes a minor portion of ore sulfides, formed due to mixing between hydrothermal fluid and seawater, resulting in cooling and neutralization, and leading to rapid precipitation of very fine-grained sulfides, framboids ($< 6 \mu\text{m}$ in size) and spherulites from the reduced water column (anoxic to dysoxic environment) on the seafloor in the bedded ore. On the other hand, framboids are replaced by later generations of sulfide minerals, especially galena and coarse-grained sphalerite, formed below the seafloor, which has been reported in various VMS, SHMS, and Irish-type deposits.

The replacement of framboidal pyrite by the later sulfides indicates the incidence of 'refining processes' during the mineralization of these deposits (Piercey, 2015; Rajabi et al., 2020). Piercey (2015) considers framboidal pyrite to be restricted to deposits formed below or near the sea floor. Mineralization in these deposits occurs in the reactive and permeable parts of the sediments under the sea floor, which is illustrated by the association of framboidal pyrite along with fine-grained galena and sphalerite.

Table 3. Characteristics of pyrite framboids in some selected sediment-hosted ore deposits

Ore Deposit Type	Host Rock	Example	Pyrite Frambooid Existence in Ore	Pyrite Frambooid characteristics
Shale-Hosted Massive Sulfide (SHMS) Zn-Pb	Early Cambrian Black Shale and Siltstone	Koushk, Chahmir, Zarigan,	Very common	Very fine-grained small framboids (geometric mean $2.7\text{--}2.9 \mu\text{m}$), abundant spherulites in the presence of organic matter
	Middle-Late Jurassic black siltstone	Hossein-Abad, Ab-Bagh and Western Haft-Savaran	Very common	fine-grained small framboids (geometric mean $4.8 \mu\text{m}$) with some larger framboids, and crystalline pyrite.
Irish Type	Early Cretaceous dolomitic limestone, dolomite and siltstone	Mehdiabad, Farahabad, Mansourabad, Anjireh-Tiran, Robat, Lakan, Eastern Haft-Savaran, Irankuh	Common	Geometric mean $7\text{--}10 \mu\text{m}$ with some larger framboids, and crystalline pyrite.
Orogenic-related Mississippi Valley Type (MVT)	Middle Triassic dolomitic limestone and dolomite	Ab-Bid, Tarz, Ahmadabad, Talkhab, and Zenoghan	Absent	No framboids, with rare pyrite crystals in host carbonates.
sediment-hosted stratabound copper (SSC)	Late Jurassic sandstones	Markesheh, Bagh-Pahlevan, Esmaeil-Abad, Kuh-e-Sargerd	Moderately common	Framboids are moderately common to rare with a broad range of sizes ($9\text{--}50 \mu\text{m}$).
	Eocene-Oligocene and Miocene sandstones	Chahbouk and Ark	Moderately common	

A study of mineralization textures, specially framboidal pyrite as a common texture in sediment-hosted Zn-Pb deposits of Iran and comparing them with similar deposits in the world shows that this texture can be observed only in deposits that mineralization occurs during sedimentation to diagenesis of the host rock. This texture is not found in typical orogenic-related MVT deposits (such as Talkhab and Ab-Bid).

Conclusion

Pyrite framboids are very common in organic matter-rich, reduced sedimentary environments. They form by the rapid crystallization of pyrite in the form of spherical microbodies under anoxic to lower dysoxic conditions. However, unattached framboids form in euxinic environments, but in the presence of high content of organic matter, especially in black shales, spherulitic pyrite can predominate over framboids, even though their physicochemical formation conditions are the same. In addition to the sedimentary environments, framboids are common in some ore deposits that form in sedimentary and volcano-sedimentary sequences (e.g., VMS, SHMS, SSC, Irish-type, sandstone-hosted Pb-Zn, sandstone-hosted U), but they are absent or rare in some other sediment-hosted ore deposits (e.g., MVT). Pyrite framboids are common in low-pyrite SHMS, VMS, SSC, sandstone-hosted Zn-Pb and U, Irish-type ore deposits, and coal deposits, but spherulitic pyrite (along with framboids) are common in Cambrian pyrite-rich SHMS Zn-Pb deposits hosted in black shales.

The recognition of different textural types of pyrite framboids and spherulites, and their relationship with other sulfide minerals are significant in determining the time of formation of many sedimentary ore deposits, especially in SH Zn-Pb mineralization. Although most framboidal pyrites have a sedimentary origin, in some ore deposits (e.g., Koushk, Chahmir, Zarigan, Hossein-Abad, Eastern Haft-Savaran, Tiran, and Irankuh), where they are associated with fine-grained sphalerite and galena, hydrothermal fluid inputs have a role in the framboids formation.

Acknowledgements

The clarity of the paper was substantially improved by the constructive reviews of Prof. David Rickard and one anonymous reviewer, and the editorial suggestions of Prof. A. Kananian.

References

- Afzal, P., Farhadi, S., Boveiri Konari, M., Shamseddin Meigooni, M., Daneshvar Saein, L., 2022. Geochemical anomaly detection in the Irankuh District using Hybrid Machine learning technique and fractal modelling. *Geopersia*, 12(1): 191-199.
- Aghanabati A., 1998. Major sedimentary and structural units of Iran (map). *Journal of Geoscience*, 7: 29-30
- Berner, R.A., 1970. Sedimentary pyrite formation. *American journal of science*, 268(1): 1-23.
- Bond, D.P., Wignall, P.B., 2010. Pyrite framboid study of marine Permian–Triassic boundary sections: a complex anoxic event and its relationship to contemporaneous mass extinction. *Geological Society of America Bulletin*, 122 (7-8): 1265-1279.
- Boveiri-Konari, M., Rastad, E., Peter, J.M., 2017. A sub-seafloor hydrothermal synsedimentary to early diagenetic origin for the Gushfil Zn-Pb-(Ag-Ba) deposit, south Esfahan, Iran. *Journal of Mineralogy and Geochemistry*, 194: 61-90.
- Boveiri Konari, M., Rastad, E., 2018. Nature and origin of dolomitization associated with sulphide mineralization: new insights from the Tappehsorkh Zn-Pb (-Ag-Ba) deposit, Irankuh Mining District, Iran. *Geological Journal*, 53(1): 1-21.
- Calvert, S.E., Pedersen, T.F., 1993. Geochemistry of recent oxic and anoxic marine sediments: implications for the geological record. *Marine geology*, 113(1-2): 67-88.

- Canfield, D.E., Berner, R.A., 1987. Dissolution and pyritization of magnetite in anoxic marine sediments. *Geochimica et Cosmochimica Acta*, 51(3): 645-659.
- Degens, E.T., Okada, H., Honjo, S., Hathaway, J.C., 1972. Microcrystalline sphalerite in resin globules suspended in Lake Kivu, East Africa. *Mineralium Deposita*, 7, 1-12.
- England, B., Ostwald, J., 1993. Framboid-derived structures in some Tasman fold belt base-metal sulphide deposits, New South Wales, Australia. *Ore Geology Reviews*, 7 (5): 381-412.
- Formolo, M.J., Lyons, T.W., 2007. Accumulation and preservation of reworked marine pyrite beneath an oxygen-rich Devonian atmosphere: Constraints from sulfur isotopes and framboid textures. *Journal of Sedimentary Research*, 77 (8): 623-633.
- Gadd, M.G., Layton-Matthews, D., Peter, J., Paradis, S., 2016. The world-class Howard's Pass SEDEX Zn-Pb district, Selwyn Basin, Yukon. Part I: trace element compositions of pyrite record input of hydrothermal, diagenetic, and metamorphic fluids to mineralization. *Mineralium Deposita*, 51 (3): 319-342.
- Galleo-Torres, D., Reolid, M., Nieto-Moreno, V., Martínez-Casado, F.J., 2015. Pyrite framboid size distribution as a record for relative variations in sedimentation rate: An example on the Toarcian Oceanic Anoxic Event in Southiberian Palaeomargin. *Sedimentary geology*, 330: 59-73. <https://doi.org/10.1016/j.sedgeo.2015.09.013>.
- Hoffman, D.L., Algeo, T.J., Maynard, J.B., Joachimski, M.M., Hower, J.C., Jaminski, J., 1998. Regional and stratigraphic variation in bottom water anoxia in offshore core shales of Upper Pennsylvanian cyclothems from the Eastern Midcontinent Shelf (Kansas), USA. *Shales and Mudstones*, 1: 243-269.
- Jakobsen, R., Postma, D., 1999. Redox zoning, rates of sulfate reduction and interactions with Fe-reduction and methanogenesis in a shallow sandy aquifer, Rømø, Denmark. *Geochimica et Cosmochimica Acta*, 63(1): 137-151.
- James, R.H., Elderfield, H., 1996. Chemistry of ore-forming fluids and mineral formation rates in an active hydrothermal sulfide deposit on the Mid-Atlantic Ridge. *Geology*, 24 (12): 1147-1150.
- Jones, B., Manning, D.A., 1994. Comparison of geochemical indices used for the interpretation of paleo-redox conditions in ancient mudstones. *Chemical Geology*, 111(1-4): 111-129.
- Khan Mohammadi, G., Rajabi, A., Niroomand, S., Mahmoodi, P., Canet, C., Alfonso, P., 2023. Carbonate-hosted Zn-Pb-Cu-Ba (-Ag) mineralization in the Mehdiabad deposit, Iran: new insights, new discoveries. In: Andrew, C.J., Hitzman, M.W., Stanley, G. (Eds.), *Irish-type Deposits around the world*. Irish Association for Economic Geology, Dublin, 545-556. DOI: <https://doi.org/10.61153/ZZWJ5211>
- Kibek, B., 1975. The origin of framboidal pyrite as a surface effect of Sulphur grains. *Mineralium Deposita*, 10(4): 389-396.
- Large, R.R., Bull, S.W., Cooke, D.R., McGoldrick, P.J., 1998. A genetic model for the HYC Deposit, Australia; based on regional sedimentology, geochemistry, and sulfide-sediment relationships. *Economic Geology* 93 (8): 1345-1368.
- Liu, K., Huang, F., Gao, S., Zhang, Z., Ren, Y., An, B., 2022. Morphology of framboidal pyrite and its textural evolution: Evidence from the Logatchev area, Mid-Atlantic Ridge. *Ore Geology Reviews*, 141: 104630.
- Liu, Z., Chen, D., Zhang, J., Lü, X., Wang, Z., Liao, W., Shi, X., Tang, J., Xie, G., 2019. Pyrite morphology as an indicator of paleo-redox conditions and shale gas content of the Longmaxi and Wufeng shales in the middle Yangtze area, south China. *Minerals*, 9(7): 428. <http://dx.doi.org/10.3390/min9070428>
- Lougheed, M.S., Mancuso, J.J., 1973. Hematite framboids in the negaunee iron formation, Michigan; evidence for their Biogenic Origin. *Economic geology*, 68(2): 202-209.
- Love, L., 1967. Early diagenetic iron sulphide in recent sediments of the Wash (England). *Sedimentology*, 9 (4): 327-352.
- Love, L., 1971. Early diagenetic polyframboidal pyrite, primary and redeposited, from the Wenlockian Denbigh Grit Group, Conway, North Wales, UK. *Journal Sedimentary Research*, 41: 1038-1044.
- Love, L., Amstutz, G.C., 1969. Framboidal pyrite in two andesites. *News Jahrb Mineral Monatsh*, 3: 97-108.
- Mahdavi, A., Rajabi, A., 2023. Neotocite textures as a clue to the exploration of Red Bed type sediment-hosted stratabound copper (SSC) deposits—evidence from Ravar–Tabas–Eshghabad copper belt, Central Iran. *International Geology Review*, (in press). <https://doi.org/10.1080/00206814>.

- 2023.2241069
- Magnall, J.M., Gleeson, S.A., Stern, R.A., Newton, R.J., Poulton, S.W., Paradis, S., 2016. Open system sulphate reduction in a diagenetic environment—Isotopic analysis of barite ($\delta^{34}\text{S}$ and $\delta^{18}\text{O}$) and pyrite ($\delta^{34}\text{S}$) from the Tom and Jason Late Devonian Zn–Pb–Ba deposits, Selwyn Basin, Canada. *Geochimica et Cosmochimica Acta*, 180: 146-163.
- Mahdavi, A., 2008. Geological, Mineralogical, Geochemical and Genesis of Markesheh Copper Deposit, Northwest of Ravar, Kerman. M. Sc Thesis, Tarbiat Modares University of Tehran, Iran: 188 pp. (in Persian with English abstract).
- Mahdavi, A., Rastad, A., Hosseini Barzy, M., 2011. Mineralogy, structure and texture and genesis of sedimentary diagenetic Cu Markeshe, Redbed type, in the Garedu Red Formation, Jurassic, south of Central Iran. *Scientific Quarterly Journal of Geosciences*, 21(81): 81-92.
- Mahmoodi, P., Peter, J.M., Rajabi, A., Rastad, E., 2023. Geological and textural characteristics as evidence for Irish-type mineralization in the Eastern Haft-Savaran deposit in: Andrew, C.J., Hitzman, M.W., Stanley, G. (Eds.), *Irish-type Deposits around the world*, Irish Association for Economic Geology, Dublin, 533-544. DOI: <https://doi.org/10.61153/PXZE7581>
- Mahmoodi, P., Rastad, E., Rajabi, A., Alfonso, P., Canet, C. Peter, J.M., 2021. Genetic model for Jurassic shale-hosted Zn-Pb deposits of the Arak Mining District, Malayer-Esfahan metallogenic belt: Insight from sedimentological, textural, and stable isotope characteristics. *Ore Geology Reviews*, 136: 104262. <https://doi.org/10.1016/j.oregeorev.2021.104262>
- Mahmoodi, P., Rastad, E., Rajabi, A., Moradpour, M., 2019. Mineralization horizons, structure and texture, alteration and mineralization stages in the Zn-Pb (Ba) Eastern Haft-Savaran deposit in Malayer-Esfahan metallogenic belt, south of Khomain. *Scientific Quarterly Journal of Geosciences*, 28(110): 3-12. <https://doi.org/10.22071/gsj.2017.91866.1192>
- Mahmoodi, P., Rastad, E., Rajabi, A., Peter, J., 2018. Ore facies, mineral chemical and fluid inclusion characteristics of the Hossein-Abad and Western Haft-Savaran sediment-hosted Zn-Pb deposits, Arak Mining District, Iran. *Ore Geology Reviews*, 95: 342-365. <https://doi.org/10.1016/j.oregeorev.2018.02.036>
- Menon, K.K., 1967. Origin of diagenetic pyrite in the Quilon Limestone, Kerala, India. *Nature*, 213(5082): 1219-1220.
- Middelburg, J.J., De Lange, G.J., Van Der Sloot, H.A., Van Emburg, P.R., Sophiah, S., 1988. Particulate manganese and iron framboids in Kau Bay, Halmahera (eastern Indonesia). *Marine Chemistry*, 23(3-4): 353-364.
- Movahednia, M., Rastad, E., Rajabi, A., Maghfouri, S., González, F. J., Alfonso, P., Choulet, F., Canet, C., 2020a. The Ab-Bagh Late Jurassic-Early Cretaceous sediment-hosted Zn-Pb deposit, Sanandaj-Sirjan zone of Iran: ore geology, fluid inclusions and (S–Sr) isotopes. *Ore geology reviews*, 121: 103484. <https://doi.org/10.1016/j.oregeorev.2020.103484>
- Movahednia, M., Rastad, E., Rajabi, A., González Sanz, F.J., 2020b. Elemental zonation and geochemistry of sulphide ore of the Ab-Bagh sedimentary-exhalative Zn-Pb deposit, southeastern margin of the Malayer-Esfahan metallogenic belt. *Researches in Earth Sciences*, 11(1): 72-88. <https://doi.org/10.52547/esrj.11.1.72>
- Ohfuji, H., Boyle, A.P., Prior, D.J., Rickard, D., 2005. Structure of framboidal pyrite: An electron backscatter diffraction study. *American Mineralogist*, 90(11-12): 1693-1704. <https://doi.org/10.2138/am.2005.1829>
- Ohfuji, H., Rickard, D., 2005. Experimental syntheses of framboids review. *Earth-Science Reviews*, 71(3-4): 147-170.
- Piercey, S.J., 2015. A semipermeable interface model for the genesis of seafloor replacement-type volcanogenic massive sulfide (VMS) deposit. *Economic Geology*, 110 (7): 1655-1660.
- Piper, D.Z., Calvert, S.E., 2009. A marine biogeochemical perspective on black shale deposition. *Earth-Science Reviews*, 95(1-2): 63-96.
- Prol-Ledesma, R.M., Canet, C., Villanueva-Estrada, R.E., Ortega-Osorio, A., 2010. Morphology of pyrite in particulate matter from shallow submarine hydrothermal vents. *American Mineralogist*, 95(10): 1500-1507.
- Raiswell, R., Berner, R.A., 1985. Pyrite formation in euxinic and semi-euxinic sediments. *American Journal of Science*, 285(8): 710-724.
- Rajabi, A., 2008. Geology, mineralogy, texture and structure, geochemistry and genesis of Chahmir Zn-

- Pb deposit, south of Behabad, Yazd Province. Unpublished M. Sc. thesis, Tarbiat Modares University, Iran: 300p.
- Rajabi A., 2022. Metallogeny and geology of sediment-hosted Zn-Pb deposits of Iran. University of Tehran Press, Tehran, 602 pp.
- Rajabi, A., Mahmoodi, P., Rastad, E., Canet, C., Alfonso, P., Niroomand, S., Yarmohammadi, A., Perrnajmodin, H., Akbari, Z., 2023. An introduction to Irish-type Zn-Pb deposits in early Cretaceous carbonate rocks of Iran. In: Andrew, C.J., Hitzman, M.W., Stanley, G. (Eds.), *Irish-type Deposits around the world*. Irish Association for Economic Geology, Dublin, 511-532. DOI: <https://doi.org/10.61153/ZZUG6529>
- Rajabi, A., Rastad, E., Alfonso, P., Canet, C., 2012a. Geology, ore facies and Sulphur isotopes of the Koushk vent-proximal sedimentary-exhalative deposit, Posht-e-Badam Block, Central Iran. *International Geology Review*, 54 (14): 1635-1648. <https://doi.org/10.1080/00206814.2012.659106>
- Rajabi, A., Rastad, E., Canet, C., 2012b. Metallogeny of Cretaceous carbonate-hosted Zn–Pb deposits of Iran: geotectonic setting and data integration for future mineral exploration. *International Geology Review*, 54(14): 1649-1672. <https://doi.org/10.1080/00206814.2012.659110>
- Rajabi, A., Canet, C., Rastad, E., Alfonso, P., 2015a. Basin evolution and stratigraphic correlation of sedimentary-exhalative Zn-Pb deposits of the Early Cambrian Zarigan-Chahmir Basin, Central Iran. *Ore Geology Reviews*, 64: 328-353. <https://doi.org/10.1016/j.oregeorev.2014.07.013>
- Rajabi, A., Rastad, E., Canet, C., Alfonso, P., 2015b. The early Cambrian Chahmir shale-hosted Zn–Pb deposit, Central Iran: an example of vent-proximal SEDEX mineralization. *Mineralium Deposita*, 50 (5): 571-590. <https://doi.org/10.1007/s00126-014-0556-x>
- Rajabi, A., Mahmoodi, P., Rastad, E., Niroomand, S., Canet, C., Alfonso, P., Shabani, A.A.T. and Yarmohammadi, A., 2019a. Comments on “Dehydration of hot oceanic slab at depth 30–50 km: Key to the formation of Irankuh-Emarat Pb-Zn MVT belt, Central Iran” by Mohammad Hassan Karimpour and Martiya Sadeghi. *Journal of geochemical exploration*, 205: 106346. <https://doi.org/10.1016/j.gexplo.2019.106346>
- Rajabi, A., Mahdavi, A., Mousivand, F., Modabberi, S., Soleymani., 2019b. Metallogeny of sedimentary copper deposits associated with salt tectonic in central Iran. The 7th national conference of tectonics and structural geology of Iran, Tehran, Iran.
- Rajabi, A., Alfonso, P., Canet, C., Rastad, E., Niroomand, S., Modabberi, S., Mahmoodi, P., 2020. The world-class Koushk Zn-Pb deposit, Central Iran: A genetic model for vent-proximal shale-hosted massive sulfide (SHMS) deposits–Based on paragenesis and stable isotope geochemistry. *Ore geology reviews*, 124: 103654. <https://doi.org/10.1016/j.oregeorev.2020.103654>
- Rajabi, A., Canet, C., Alfonso, P., Mahmoodi, P., Yarmohammadi, A., Sharifi, S., Mahdavi, A., Rezaei, S., 2022. Mineralization and Structural Controls of the Ab-Bid Carbonate-Hosted Pb-Zn (\pm Cu) Deposit, Tabas-Posht e Badam Metallogenic Belt, Iran. *Minerals*, 12(1): 95.
- Rickard, D., 1970. The origin of framboids. *Lithos*, 3(3), 269-293.
- Rickard, D., 2006. The solubility of FeS. *Geochimica et Cosmochimica Acta*, 70(23): 5779-5789.
- Rickard D., 2012. Sedimentary pyrite. In: Rickard, David, (ed), *Sulfidic Sediments and Sedimentary Rocks*, Vol. 65. *Developments in Sedimentology*, Elsevier, pp. 233-285.
- Rickard D., 2019a. How long does it take a pyrite framboid to form? *Earth and Planetary Science Letters*, 513: 64-68.
- Rickard, D., 2019b. Sedimentary pyrite framboid size-frequency distributions: A meta-analysis. *Palaeogeography, Palaeoclimatology, Palaeoecology*, 522: 62-75.
- Rickard, D., 2021. *Framboids*. Oxford University Press, Londen, pp. 334.
- Rosúa, F. C., Ruano, S. M., Hach-Alí, P. F., 2003. Iron sulphides at the epithermal gold-copper deposit of Palai-Islica (Almería, SE Spain). *Mineralogical Magazine*, 67(5): 1059-1080.
- Rust, G.W., 1935. Colloidal primary copper ores at Cornwall Mines, southeastern Missouri. *The Journal of Geology*, 43 (4): 398-426.
- Sáez, R., Moreno, C., González, F., Almodóvar, G.R., 2011. Black shales and massive sulfide deposits: causal or casual relationships? Insights from Rammelsberg, Tharsis, and Draa Sfar. *Mineralium Deposita*, 46: 585-614.
- Sawlowicz, Z., 1990. Primary copper sulphides from the Kupferschiefer, Poland. *Mineralium Deposita*, 25(4): 262-271.
- Sawlowicz, Z. 1993. Pyrite framboids and their development: a new conceptual mechanism.

- Geologische Rundschau 82 (1): 148-156.
- Sawłowicz, Z., 2000. Frambooids: from their origin to application. *Mineralogical Transactions*, 88: 80 pp.
- Scott, R.J., Meffre, S., Woodhead, J., Gilbert, S.E., Berry, R.F., Emsbo, P., 2009. Development of framboidal pyrite during diagenesis, low-grade regional metamorphism, and hydrothermal alteration. *Economic Geology*, 104(8): 1143-1168.
- Skei, J.M., 1988. Formation of framboidal iron sulfide in the water of a permanently anoxic fjord-Framvaren, South Norway. *Marine Chemistry*, 23(3-4): 345-352.
- Steinike, K., 1963. A further remark on biogenic sulfides; inorganic pyrite spheres. *Economic Geology*, 58(6): 998-1000.
- Stene, L.P., 1979. Polyframboidal pyrite in the tills of southwestern Alberta. *Canadian Journal of Earth Sciences*, 16 (10): 2053-2057.
- Suits, N. S., Wilkin, R. T., 1998. Pyrite formation in the water column and sediments of a meromictic lake. *Geology*, 26(12): 1099-1102.
- Suk, D., Peacor, D.R., der Voo, R.V., 1990. Replacement of pyrite framboids by magnetite in limestone and implications for palaeomagnetism. *Nature*, 345(6276): 611-613.
- Taylor, G.R., 1982. A mechanism for framboid formation as illustrated by a volcanic exhalative sediment. *Mineralium Deposita*, 17(1): 23-36.
- Wignall, P. B., Newton, R., Brookfield, M. E., 2005. Pyrite framboid evidence for oxygen-poor deposition during the Permian–Triassic crisis in Kashmir. *Palaeogeography, Palaeoclimatology, Palaeoecology*, 216(3-4): 183-188.
- Wignall, P., Newton, R., 1998. Pyrite framboid diameter as a measure of oxygen deficiency in ancient mud rocks. *American Journal of Science*, 298 (7): 537-552.
- Wilkin, R.T., Barnes, H., 1997. Formation processes of framboidal pyrite, *Geochimica et Cosmochimica Acta*, 61 (2): 323-339.
- Wilkin, R.T., Barnes, H.L., Brantley, S.L., 1996. The size distribution of framboidal pyrite in modern sediments: an indicator of redox conditions, *Geochimica et Cosmochimica Acta*, 60 (20): 3897-3912.
- Wilkinson, J.J., 2003. On diagenesis, dolomitisation, and mineralisation in the Irish Zn-Pb ore field. *Mineralium Deposita*, 38(8): 968-983.
- Wilkinson, J.J., Eyre, S.L., Boyce, A.J., 2005. Ore-forming processes in Irish-type carbonate-hosted Zn-Pb deposits: Evidence from mineralogy, chemistry, and isotopic composition of sulfides at the Lisheen mine. *Economic Geology*, 100(1): 63-86.
- Xu, G., Hannah, J.L., Bingen, B., Georgiev, S., Stein, H.J., 2012. Digestion methods for trace element measurements in shales: Paleo-redox proxies examined. *Chemical Geology*, 324: 132-147.
- Yarmohammadi, A., Rastad, E., Rajabi, A., 2016. Geochemistry, fluid inclusion study, and genesis of the sediment-hosted Zn-Pb (\pm Ag \pm Cu) deposits of the Tiran basin, NW of Esfahan, Iran. *Journal of Mineralogy and Geochemistry*, 193 (2): 183-203.
- Yesares, L., Drummond, D.A., Hollis, S.P., Doran, A.L., Menuge, J.F., Boyce, A.J., ... Ashton, J.H., 2019. Coupling mineralogy, textures, stable and radiogenic isotopes in identifying ore-forming processes in Irish-type carbonate-hosted Zn–Pb deposits. *Minerals*, 9(6): 335.
- Zhao, J., Liang, J., Long, X., Li, J., Xiang, Q., Zhang, J., Hao, J., 2018. Genesis and evolution of framboidal pyrite and its implications for the ore-forming process of Carlin-style gold deposits, southwestern China. *Ore Geology Reviews*, 102: 426-436.

